*Journal of The Electrochemical Society*, **162** (9) G82-G86 (2015)
0013-4651/2015/162(9)/G82/5/$33.00 © The Electrochemical Society

# Non-Competitive Reversible Inhibition of Laccase by $H_2O_2$ in Osmium Mediated Layer-By-Layer Multilayer $O_2$ Biocathodes

**Matteo Grattieri,[*,a,b] Pablo Scodeller,[c] Catherine Adam, and Ernesto J. Calvo[z]**

*INQUIMAE-DQIAyQF, Facultad de Ciencias Exactas y Naturales, Universidad de Buenos Aires, Argentina, 1428 Buenos Aires, Argentina*

A systematic study of the inhibition of laccase by hydrogen peroxide in oxygen biocathodes composed of layer-by-layer self-assembled multilayers of *Trametes-trogii* laccase and osmium derivatized poly(allylamine) redox mediator has been accomplished using a rotating disc electrode at different electrode potentials, oxygen partial pressures and hydrogen peroxide concentrations. The experimental results are consistent with a reversible non-competitive inhibition mechanism in agreement with the Solomon mechanism for laccase previously reported.


Manuscript submitted May 20, 2015; revised manuscript received June 16, 2015. Published July 9, 2015.

The multicopper enzyme laccase (EC1.10.3.2; benzenediol: oxygen oxido-reductase) is an extracellular blue copper enzyme in plants and fungi which catalyzes the oxidation of biphenols and the four-electron reduction of molecular oxygen to water. It contains four copper atoms, denoted T1, T2 and T3 according to their spectroscopic properties. In high potential laccases the copper center T1 can be reduced by phenol compounds,[1] one-electron redox mediators[2–4] and direct electron transfer from electrodes.[5–8] While substrates are oxidized at T1 copper site, further internal electron transfer leads to the reduction of molecular $O_2$ at the trinuclear T2/T3 cluster.[9,10]

The catalytic ability of laccases to activate the $O_2$ 4-electron reduction under physiological conditions at unprecedented high electrode potentials (c.a. 0.60 V vs. Ag/AgCl) has encouraged their study in cathodes for bio-fuel cells and an extensive literature on the electrochemistry of laccases from different sources has followed in recent years.[3,11–13]

In order to achieve reproducible enzyme electrodes, it is essential to control film thickness, enzyme and mediator surface loading, variation of oxygen partial pressure, convective-diffusion mass transport in the liquid electrolyte, and the charge of the topmost layer.[14,15] This can be achieved by using the layer-by-layer electrostatic adsorption technique pioneered by Decher.[16] The advantage of the LbL self-assembly over hydrogels of same composition is that the electrodes can be designed and built choosing from different variables such as thickness, enzyme loading, osmium concentration and charge of the topmost layer. Unlike randomly oriented redox hydrogels, cast or electropolymerized films, organized nanostructured thin films allow control over the film thickness, the enzyme loading and the mediator concentration. While one assumes homogeneous composition in the x-y plane at any normal distance z from the metal surface, there is a normal distribution of species, electrostatic potential and vector electron transfer given by a redox concentration gradient. LbL laccase (Lac) and osmium poly(allylamine) multilayers, $(Lac)_n(PAH\text{-}Os)_m$, have been characterized by ellipsometry, quartz crystal microbalance, cyclic voltammetry,[4,17,18] XPS,[19] etc.

In 2010 our research group reported the first evidence that laccase could be inhibited by $H_2O_2$ produced by the enzymatic reduction of oxygen in osmium mediated electron transfer.[4] Subsequently Minteer's group reported on the inhibition of laccase in biofuel cells with glucose anodes that produced peroxide.[20] Furthermore, Milton and Minteer[21] have recently reported the reversible inhibition of laccase by hydrogen peroxide both under direct electron transfer (DET) and mediated by (2,2′-azino-bis(3-ethylbenzothiazoline-6-sulfonic acid) ABTS. Since hydrogen peroxide can be formed at the anodes of biofuel cells and also be accumulated during oxygen reduction in laccase modified electrodes, it is imperative to understand the mechanism of inhibition.

In the present report we extend the previous work with *Trametes trogii* laccase[4,18] self-assembled layer-by-layer by sequential electrostatic adsorption of the redox mediator polyelectrolyte PAH-Os and laccase on mercaptopropanesulfonate (MPS) thiolated gold surfaces, and systematically study the inhibition of the enzyme in the $O_2$ biocathodes by $H_2O_2$.

## Experimental

Purified enzyme laccase from *Trametes-trogii* has been employed in this study.[22] Strain 463 (BAFC: Mycological Culture Collection of the Department of Biological Sciences, Faculty of Exact and Natural Sciences, University of Buenos Aires) of *Trametes-trogii* (Funalia-trogii) (Polyporaceae, Aphyllo phora-les, Basidiomycetes) was used in these experiments. Stock cultures were maintained on malt extract agar slants at 4°C. Details of culture conditions and purification of the enzyme laccase have been reported elsewhere.[4] 3-mercaptopropane sulfonate (MPS) was purchased from Sigma-Aldrich Argentina. Poly(allylamine) (PAH), sodium acetate and acetic acid (100%) were obtained from Fluka. All reagents were analytical grade and used without further purification except PAH which was dialyzed against Milli-Q water. Ultra pure water was obtained from a Milli-Q purification system (nominal resistivity 18.2 MΩ at 25°C) and used to prepare all solutions.

The complex osmium poly(allylamine) (PAH-Os) was synthesized as described elsewhere.[23] The osmium content was evaluated spectrophotometrically at $\lambda = 475$ nm ($\varepsilon = 8100\ M^{-1} \cdot cm^{-1}$).

A gold electrode primed with 20 mM 3-mercaptopropane sulfonate in 0.01 M $H_2SO_4$ was further modified on top with a layer of Os bipyridine covalently tethered to poly(allylamine) cationic polyelectrolyte followed by adsorption of laccase from a solution of a suitable pH value (around 5) where the protein carries a net negative charge (pI = 3.3). This process was repeated with rinsing between each adsorption step to yield an all-integrated enzyme-mediator system as previously reported.[18] The enzyme laccase (Lac) was co-immobilized with 100 μL of 0.44 mM osmium bipyridine redox polyelectrolyte mediator (PAH-Os, pH 8) via layer-by-layer (LbL) electrostatic self-assembly technique. After rinsing the electrode with Milli-Q water, the following layer was deposited covering the modified electrode with 100 μL of 8 μM laccase solution in Milli-Q water for 20 minutes. In every case we covered the LbL self-assembled electrode structures with a topmost layer of PAH-Os.

*Electrochemistry.*— Cyclic voltammetry was performed using an Autolab PGSTAT 30 potentiostat in a three-electrode cell with a platinum gauze as counter electrode and Ag/AgCl/3 M as reference electrode (all potentials herein are referred to this reference electrode).

*Electrochemical Society Student Member.
[a]Present Address: Department of Chemistry, Materials and Chemical-Engineering, Politecnico di Milano, 20133 Milan, Italy.
[b]Present Address: Department of Chemistry, Università degli Studi di Milano, 20133 Milan, Italy.
[c]Present Address: Institute of Biomedicine and Translational Medicine, University of Tartu, 50411 Tartu, Estonia.
[z]E-mail: calvo@qi.fcen.uba.ar

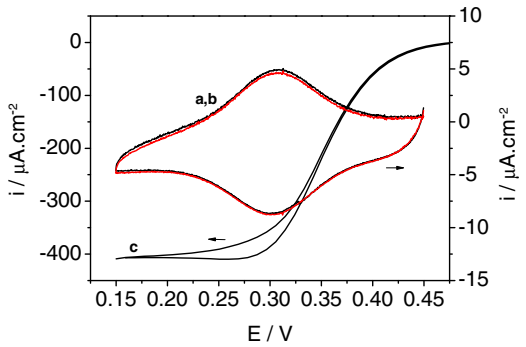


**Figure 1.** Cyclic Voltammetry of $(Lac)_3(PAH\text{-}Os)_4$ biocathode in 0.1 M acetate buffer (pH 4.7) + 0.2 M $KNO_3$ in absence of oxygen (curve a and b), and at $pO_2 = 1$ atm (curve c), without $H_2O_2$ (curves a,c) and with 1 mM $H_2O_2$ (curve b). The right axis corresponds to curves a,b and the left axis to curve c.

The working electrodes were rotating gold discs (d = 5 mm) embedded in KelF polymer. All measurements were performed in 0.1 M acetate buffer of pH 4.7 containing 0.2 M $KNO_3$.

Before measurements, all solutions were degassed with pure nitrogen or saturated with gas mixtures of nitrogen/oxygen in different ratios. In order to control the oxygen partial pressure, the $N_2/O_2$ ratio of this gas mixture was controlled by means of precision flow meters and flow regulators (G. Bruno Schilling, Argentina). Calibration of the $O_2/N_2$ gas mixtures was performed with the rotating disc electrode (RDE) convective-diffusion limiting current density.

## Results

The adsorption of Laccase on the PAH-Os layers was monitored with the quartz crystal microbalance obtaining an average surface concentration of $1.34 \times 10^{-11}$ mol. $cm^{-2}$ in each adsorption step, while the thickness of the enzyme-mediator multilayer thin films was monitored by in-situ ellipsometry at 632 nm. As shown by XPS,[19] the enzyme multilayer films are comprised of alternate layers of Lac and osmium polyelectrolyte mediator with some intermixing and interpenetration of the layers contributing to a flexible wiring of the enzyme due to segmental motion and electron hopping between adjacent redox centers and the enzyme Cu(T1) center.[4,24]

Figure 1 depicts the electrochemical response of the biocathode in absence and presence of oxygen. Under anaerobic conditions, the characteristic redox wave due to the surface confined osmium complex can be clearly indentified. In presence of oxygen, the Nerstian shape of the laccase mediated $O_2$ reduction catalytic current clearly develops.

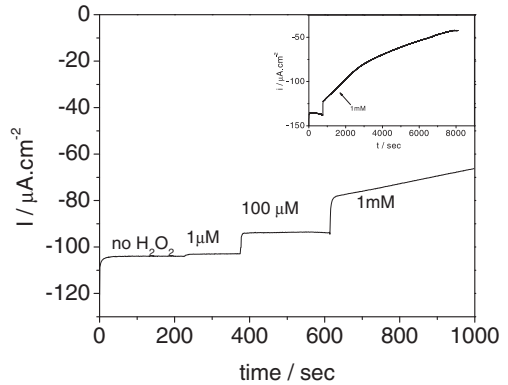


**Figure 2.** Chronoamperometry of $(Lac)_3(PAH\text{-}Os)_4$ biocathode at $pO_2 = 0.2$ atm with added $H_2O_2$ in 0.1 M acetate buffer (pH 4.7) + 0.2 M $KNO_3$ at E = 0.15 V, RDE: w = 16 Hz. Inset: expanded plot for 1 mM.

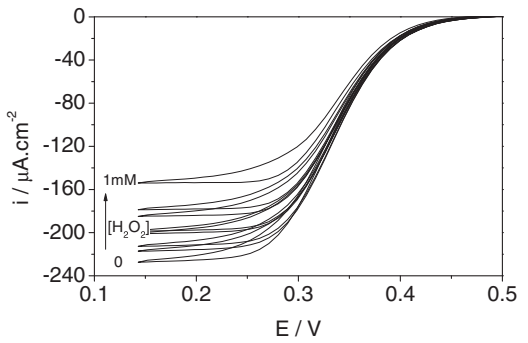


**Figure 3.** Cyclic Voltammetry of $(Lac)_3(PAH\text{-}Os)_4$ at different $H_2O_2$ concentrations (0, 1, 10, 50, 100, 250, 500 and 1000 µM) for $pO_2 = 1.00$ atm in 0.1 M acetate buffer (pH 4.7) + 0.2 M $KNO_3$ at 25 $mVs^{-1}$, RDE: w = 16 Hz.

Figure 2 shows the $O_2$ reduction current evolution after addition of $H_2O_2$ from 1 µM to 1 mM final concentrations. In all cases, the current drops to a steady state value at each peroxide concentration. Notice in the inset that for the highest peroxide concentration a steady current density value is reached after more than two hours. This result is indicative of a reversible inhibition by peroxide since a steady state current arises from a balance between the inhibition rate, which increases with peroxide concentration, and the rate of the enzyme inhibitor release. Irreversible enzyme inhibition would result in a drop to zero of the catalytic $O_2$ reduction current at all peroxide concentrations.

Thus at each peroxide concentration a fraction of the enzyme molecules is inactivated while there is a population of remaining active enzyme for each inhibitor concentration.

Figure 3 depicts current density-potential curves for the enzymatic reduction of oxygen mediated by the osmium polymer at different peroxide concentrations. The Nernstian potential dependence is identical with and without peroxide in solution and the decrease in the catalytic current is proportional to the peroxide concentration.

Larger inhibition is observed at higher oxygen partial pressures as can be seen in linear Dixon plots of Figure 4 with a decrease in the slopes at higher $pO_2$.

Linearity of Dixon plots indicates that the enzyme-inhibitor complex cannot reduce oxygen (complete inhibition).[25] It should be noticed that for thin films the current density is proportional to the enzyme reaction rate since diffusion effects are negligible in ultra thin films (see below).

A complete set of catalytic waves at increasing inhibitor concentrations is shown in Figure 5 as a function of the oxygen partial pressure.

The curves have been normalized to the limiting current at $pO_2 = 1.00$ atm in peroxide free solution, c.a. 114 µA. $cm^{-2}$. The data was collected at 0.15 V where the complete reduction of the Os polymer can be reached.

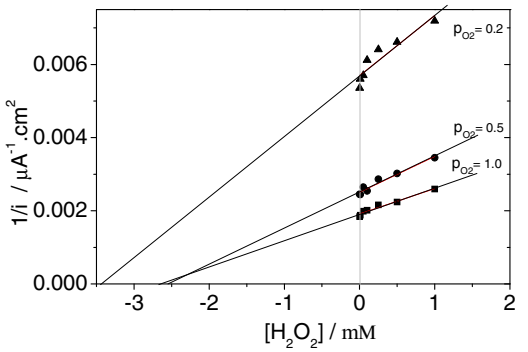


**Figure 4.** Dixon plot 1/i vs. $[H_2O_2]$ for $pO_2$ = 0.2, 0.5 and 1.00 for $(Lac)_3(PAH\text{-}Os)_4$ biocathode.

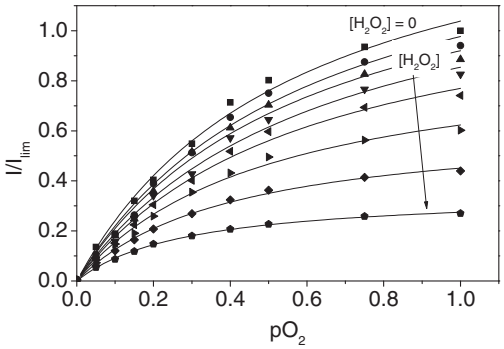


**Figure 5.** Normalized $O_2$ reduction catalytic currents at different peroxide concentrations (0, 1, 10, 50, 100, 250, 500 and 1000 μM) at E = 0.15 V, RDE: w = 16 Hz. Lines are best fit to Eq. 10.

For each peroxide concentration, the $O_2$ reduction bio-catalytic current density increases with oxygen concentration as it does in the absence of the inhibitor. The larger the concentration of peroxide in solution, the lower the bio-cathode current density. However, in all cases the characteristic enzyme electrode response is maintained.

The reversible inhibition of laccase biocatalytic oxygen reduction by peroxide results in a decrease of $i_{max}$ and the apparent Michaelis Menten constant, $K_{O2}$ = 0.5–0.6 atm, c.a. below 250 μM. In order to determine the type of inhibition on the catalytic current, the complex interplay between diffusion and non-linear enzyme kinetics needs to be taken into account, since the current density is not necessarily proportional to the rate of the enzyme reaction. This is discussed in the next section.

## Discussion

During the catalytic reduction of oxygen by laccase mediated by the osmium complex tethered to the poly-electrolyte, PAH-Os, the reactions occurring in the film can be written as:[4]

$$4PAH\text{-}Os\,(II) + \text{Lac}\,[4\text{Cu(II)}] \xrightarrow{k} \text{Lac}\,[4\text{Cu(I)}] + 4PAH\text{-}Os\,(III) \quad [1]$$

$$\text{Lac}\,[4\text{Cu(I)}] + O_2 + 4H^+ \underset{}{\overset{K_{M,S}}{\rightleftharpoons}} \text{ES} \xrightarrow{k_{cat}} \text{Lac}\,[4\text{Cu(II)}] + H_2O \quad [2]$$

Where ES is the complex formed between Lac and molecular oxygen.

At the electrode surface:

$$4\left\{PAH\text{-}Os\,(III) + e^-\,(electrode) \rightarrow PAH\text{-}Os\,(II)\right\} \quad [3]$$

with further redox charge propagation by electron hopping between adjacent osmium redox sites covalently bound to the polymer backbone in the normal direction to the electrode surface in the multilayer film assisted by segmental motion of the polymer strands.

In Eq. 8 the stoichiometry number is $\varsigma = 4$ since four moles of osmium complex are needed to fully reduce the 4-copper sites of Lac, while the number of electrons is n = 1 for the osmium redox mediator.[26]

The substrate $O_2$ undergoes partition between the bulk solution and the film (we assume a partition coefficient $K_S = 1$ for oxygen since the thin enzyme films are highly hydrated) and then diffuses within the film with a diffusion coefficient $D_{O2}$. The mediator is assumed to be confined within the film, PAH-Os, covalently attached to the polyelectrolyte backbone. Charge propagation occurs by electron hopping self-exchange between adjacent sites of the reduced and the oxidized forms of the mediator described by a diffusion coefficient $D_e$.[27,28] Michaelis-Menten kinetics is assumed for the enzyme-substrate reaction with the association constant $K_{MS}$ and enzyme turnover, $k_{cat}$. The reduced mediator, PAH-Os(II) regenerates the enzyme from the "Native Intermediate", NI, into the "Fully Reduced Laccase" Lac[4 Cu(II)] and Lac[4 Cu(I)] respectively[29] by exchanging 4 electrons with a mediator-enzyme constant k, according to the conventional "ping-pong" mechanism. It should be noted that under physiological conditions these four electrons are exchanged sequentially through the T1 copper site of the enzyme and further transferred by internal electron transfer (ET) to the tri-nuclear T2-T3 cluster.[29]

The second-order differential equations describing the system in the steady state are given by Eqs. 4 and 5.[2,30] The symbols in brackets refer to the concentrations of the corresponding species which vary across the film. Equations 4 and 5 are non-linear second order differential equations and have no closed analytical solutions.

$$D_e \frac{d^2\,[\text{PAH-Os}]}{dx^2} = \frac{\xi k k_{cat}\,[\text{PAH-Os}]\,[O_2]\,[\text{Lac}]_{TOT}}{k\,[\text{PAH-Os}]\left(K_{MS} + [O_2]\right) + k_{cat}\,[O_2]} \quad [4]$$

$$D_{O_2} \frac{d^2\,[O_2]}{dx^2} = \frac{k k_{cat}\,[\text{PAH-Os}]\,[O_2]\,[\text{Lac}]_{TOT}}{k\,[\text{PAH-Os}]\left(K_{MS} + [O_2]\right) + k_{cat}\,[O_2]} \quad [5]$$

Pratt and Bartlett[30,31] have described a kinetic case-diagram for approximate solutions of the differential Eqs. 4 and 5 with the boundary conditions for multilayer enzyme electrode with self-contained immobilized redox mediator and freely diffusing enzyme-substrate (cases I to VII). These approximations have been recently verified experimentally for glucose oxidase and PAH-Os in LbL films.[32]

In LbL films, the film thickness, Os surface concentration and enzyme loading grow with the number of adsorption steps. The catalytic current varies with the film thickness since charge propagates within the film by electron hopping and the charge increases with thickness.[27]

At high bulk oxygen concentrations the model predicts that the current will be limited by the kinetics of the reaction between the mediator and the enzyme T1 Cu site, cases I and II in Bartlett-Pratt model for thin and thick films respectively.[24,25]

$$I(caseI) = \zeta n F [PAH\text{-}Os]_{TOT} k [Lac]_{TOT} L \quad [6]$$

$$I(caseII) = nF[PAH\text{-}Os]_{TOT}\sqrt{\zeta D_e k [Lac]_{TOT}} \quad [7]$$

Therefore at high oxygen concentration, the catalytic current increases linearly with the film thickness (number of enzyme bilayers), the [PAH-Os(II)] follows a Nernstian dependence on the electrode potential:

$$\ln\left[\frac{i_L}{i} - 1\right] = \frac{F\left(E - E_{1/2}\right)}{RT} \quad [8]$$

At low oxygen concentration, cases V and VII in Bartlett-Pratt model describe the biocathode current density for thin and thick films respectively:[30]

$$I(caseV) = \zeta n F \frac{L[Lac]_{TOT} k_{cat} K_S [O_2]_\infty}{K_{MS} + K_S [O_2]_\infty} \quad [9]$$

$$I(caseVII) = nF\sqrt{\frac{2\zeta D_e [PAH\text{-}Os]_{TOT} k_{cat} [Lac]_{TOT} K_S [O_2]_\infty}{K_{MS} + K_S [O_2]_\infty}} \quad [10]$$

Figure 6 depicts a plot of the catalytic current density at $pO_2$ = 1 atm at the plateau potential (0.15 V) as a function of the number of laccase layers and PAH-Os, i.e. the film thickness. For the thinnest films (corresponding to the lower coverage) the current increases linearly as the film thickness increases (case I). For the thicker films, on the other hand, the current density reaches a constant value, $i_{max}$ (case II).

This is in excellent agreement with the predictions of the model: in case I, for the thinnest films, the current dependence in film thickness is first order while for thicker films, case II predicts a current density independent of film thickness. It is noteworthy that evidence for the transition of the limiting cases of Pratt-Bartlett model for amperometric enzyme electrodes could be obtained because of the unique

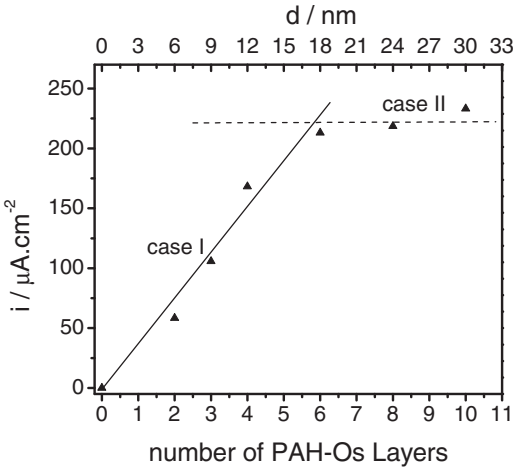


**Figure 6.** $O_2$ reduction catalytic current at 0.15 V vs. Ag/AgCl as function of number of PAH-Os/Laccase layers; measured by cyclic voltammetry (v = 5 mV/sec) in $O_2$ saturated 0.1 M acetate buffer 0.2 M $KNO_3$ pH 4.7; RDE: w = 9 Hz. Ellipsometric thickness d.

features of the LbL enzyme multilayer strategy, i.e. the ability to vary the film thickness in a controlled way at the nanometer scale.

In both cases, for the enzyme-mediator rate determining step, one expects a Nernstian dependence of the catalytic current that follows the Os(II) redox mediator concentration dependence on electrode potential (Eq. 9) giving rise to a catalytic wave in Figure 5.[30] It should be noted that $E_{1/2}$ shifts from the reversible potential of the Os(II)/Os(III) surface redox couple, 0.35 V, toward less positive potentials as the number of layers increases, approaching the redox potential of the surface Os(III)/Os(II) couple under these experimental conditions, i.e. 0.31 V.[30]

At low $O_2$ concentration with $[O_2]_\infty \ll K_{MS}$, case V predicts a Michaelis Menten dependence on $O_2$ concentration, while for case VII, a square root dependence is expected. Notice the different laccase concentration dependence for thin (Eq. 8) and thick films (Eq. 10), i.e. linear and square root respectively because of electron diffusion limitations in thick films.

We can approximate the current density to the enzyme reaction rate only for thin films (see below). Figure 7 shows different diagnostic plots for the enzyme inhibition in thin films.[25,33,34]

Linear Lineweaver Burke double reciprocal plots (Fig. 7A) with convergence on the x-axis corresponds to apparent non-competitive inhibition. However, convergence of data on the ordinate, characteristic of competitive inhibition, cannot be completely ruled out.

Parallel linear Eadie-Hofstee plots (Fig. 7B) are characteristic of non-competitive inhibition which is confirmed by the non-parallel Hanes plots (Fig. 7C).[25]

In non-competitive enzyme inhibition mechanism, the inhibitor binds to a different site than the substrate binding site.[25,34] The inhibitor may bind to the free enzyme or to the enzyme-substrate complex. Similar inhibition has been recently reported for another artificial mediator of laccase oxygen biocathodes (ABTS) by Minteer's group.[21]

Furthemore, the $(Lac)_n(PAH\text{-}Os)_m$ biocathodes do not electrochemically reduce hydrogen peroxide.[4] A comparison of the CV in the absence and presence of peroxide in solution is shown in Figure 1 under anaerobic conditions and demonstrates that $H_2O_2$ cannot be reduced by laccase since there is no difference after addition of peroxide to the electrolyte.

We unambiguously may conclude that soluble hydrogen peroxide is a non-competitive reversible inhibitor of laccase in oxygen biocathodes mediated by PAH-Os.

It should be stressed that for thick films, i.e L > 15 nm, the diagnostic plots of Figure 7 are no longer valid since the bio-catalytic current density is no longer proportional to the enzymatic rate be-

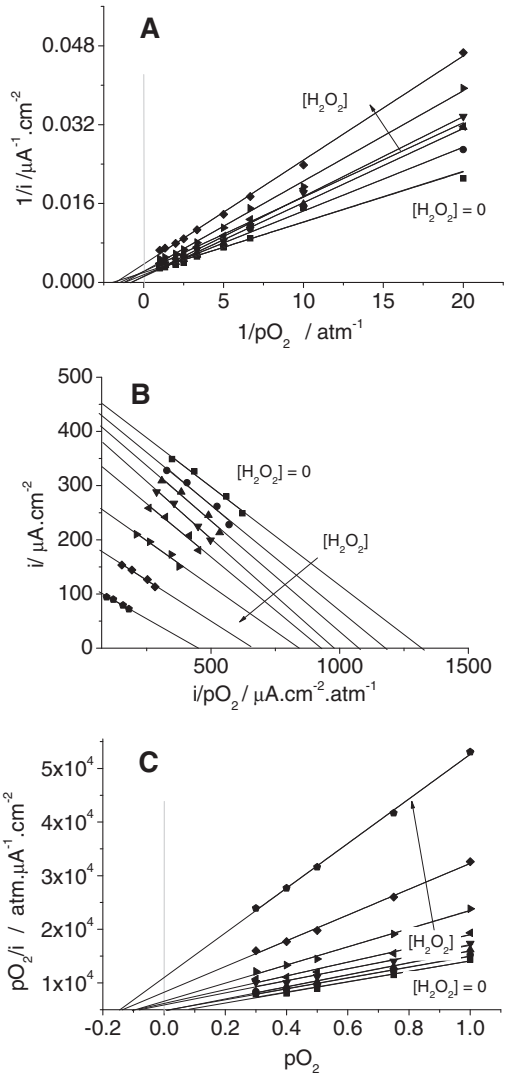


**Figure 7.** A. Lineweaver Burke plot, B. Eadie-Hofstee plot, C. Hanes plot.

cause of diffusion limitations and the current dependence on oxygen substrate, enzyme and redox mediator is given by Eq. 10.

We demonstrate this behavior with data in Figure 8 for films with 4 and 12 enzyme-redox polymer bilayers, respectively. In the absence of peroxide inhibitor the normalized current densities to the maximum current show no difference for thin and thick films. On the other hand, when 1 mM peroxide is present in the solution, the inhibited

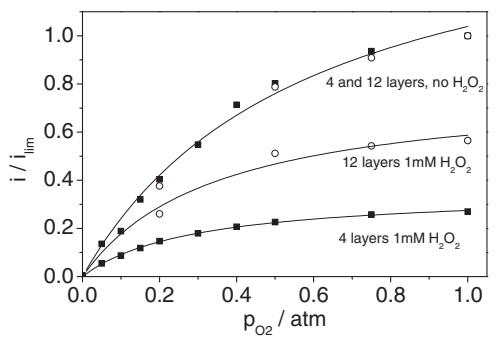


**Figure 8.** Normalized catalytic current vs. $pO_2$ for thin (■) and thick (○) films and effect of addition of 1 mM $H_2O_2$. Lines are best fit to Eq. 10.

biocathode shows a larger current drop for a thin film (4 layers) than for a thick film (12 layers). For the same fraction of inhibited enzyme molecules in the films, the current density dependence on enzyme concentration is weaker for thick films than for thin ones, i.e. $[Lac]^{1/2}$ in Eq. 11.

On the basis of the experimental evidences, we will discuss possible mechanisms to explain the reversible non-competitive inhibition of laccase oxygen biocathodes by hydrogen peroxide.

Solomon's group has extensively studied the mechanism of laccase oxygen catalysis.[9,10,29,35] Solomon's mechanism considers that oxygen binds to the fully reduced laccase forming the laccase peroxide intermediate with $O_2$ bridging between T2Cu(II) and T3Cu(II) and T3Cu(I).

In order to explain $H_2O_2$ not binding to the $O_2$ binding site, we suggest that exogenous soluble $H_2O_2$ inhibits laccase by oxidizing T3Cu(I). Previous evidence that peroxide oxidizes the CuT3 site in laccase was provided by Solomon's group,[36] and further disclosed that $H_2O_2$ binds with low affinity to the oxidized CuT2/T3 trinuclear center with the need of CuT2 center to bind peroxide,[37] previously suggested by Vanngard.[38]

Taking into account this mechanism, we have examined the inhibition reversibility. After inhibition, washing the electrode and immersing in a fresh peroxide free electrolyte we have not seen any difference with the inhibited response. However, if the inhibited electrode was reduced at −0.4 V in peroxide free and oxygen free electrolyte for ten minutes, we partially recovered the response of the original non-inhibited bio-cathode (see evidence in supporting information). This suggests that peroxide oxidizes laccase, which needs fully reduced T3Cu sites to bind $O_2$ and that strong reduction of these sites recovers the catalytic activity.

Notice that laccase activity is recovered in the absence of oxygen and that the inhibition by peroxide is more important at the highests oxygen partial pressures. Therefore we assume that in the reversible inhibition, peroxide competes for the electron injected at T1 copper center with the oxygen reduction at the trinuclear cluster and the reductive reactivation of laccase. In the absence of oxygen all electrons injected at T1 by Os(II) result in the reductive enzyme reactivation. However, at 1 mM peroxide concentration the initial response was no longer reached, which agrees with a previous study of Solomon's group who demonstrated that irreversible protein damage occurs at high $H_2O_2$ concentrations.[36]

From the present experimental evidence and previous evidence of Kau et al.[36] we suggest that peroxide inhibits laccase by oxidizing T3Cu(I) and interfering in the Solomon 4-electron biocatalytic reduction of oxygen mechanism.[35]

## Conclusions

For thin films self-assembled layer-by-layer of *Trametes-trogii* laccase and poly(allylamine) osmium (PAH-Os) redox mediator we have shown enzyme non-competitive reversible inhibition of $O_2$ biocathodes by exogenous soluble $H_2O_2$ using a rotating disc electrode at different electrode potentials, $O_2$ partial pressures and hydrogen peroxide concentrations.

The competition of inhibition, and reductive enzyme reactivation determines the steady state oxygen reduction current at each peroxide concentration, $O_2$ partial pressure and Os(II) concentration (which follows a Nernstian response of the electrode potential).

The experimental evidence presented here for the inhibition of laccase by peroxide is fully consistent with Solomon's mechanism and careful spectroscopic studies that demonstrated that $H_2O_2$ oxidizes T3Cu site of laccase.[36,37,39]

## Acknowledgment

The authors acknowledge financial support from CONICET, ANPCyT and the University of Buenos Aires (UBA). MG acknowledges Prof. S. P. Trasatti and Università degli Studi di Milano for a Ph. D Student fellowship to visit UBA. Funding Sources ANPCyT PICT 2008 No.2037. The manuscript was written through contributions of all authors. All authors have given approval to the final version of the manuscript. All authors contributed equally.

## References

1. F. Xu, W. S. Shin, S. H. Brown, J. A. Wahleithner, U. M. Sundaram, and E. I. Solomon, *Biochimica Et Biophysica Acta-Protein Structure and Molecular Enzymology*, **1292**, 303 (1996).
2. J. W. Gallaway and S. A. C. Barton, *Journal of the American Chemical Society*, **130**, 8527 (2008).
3. N. Mano, V. Soukharev, and A. Heller, *Journal of Physical Chemistry B*, **110**, 11180 (2006).
4. P. Scodeller, R. Carballo, R. Szamocki, L. Levin, F. Forchiassin, and E. J. Calvo, *Journal of the American Chemical Society*, **132**, 11132 (2010).
5. C. F. Blanford, R. S. Heath, and F. A. Armstrong, *Chemical Communications*, 1710 (2007).
6. C. E. F. C. F. Blanford, R. S. Heath, and F. A. Armstrong, in *Faraday Discussion 140: Electocatalysis – Theory and Experiment at the Interface*, A. Russell Editor, Southampton, UK (2008).
7. N. S. Parimi, Y. Umasankar, P. Atanassov, and R. P. Ramasamy, *Acs Catalysis*, **2**, 38 (2012).
8. M. Sosna, J.-M. Chretien, J. D. Kilburn, and P. N. Bartlett, *Physical Chemistry Chemical Physics*, **12**, 10018 (2010).
9. E. I. Solomon, M. J. Baldwin, and M. D. Lowery, *Chemical Reviews*, **92**, 521 (1992).
10. E. I. Solomon, U. M. Sundaram, and T. E. Machonkin, *Chemical Reviews*, **96**, 2563 (1996).
11. T. Chen, S. C. Barton, G. Binyamin, Z. Q. Gao, Y. C. Zhang, H. H. Kim, and A. Heller, *Journal of the American Chemical Society*, **123**, 8630 (2001).
12. G. T. R. Palmore and H. H. Kim, *Journal of Electroanalytical Chemistry*, **464**, 110 (1999).
13. M. R. Tarasevich, V. A. Bogdanovskaya, and L. N. Kuznetsova, *Russian Journal of Electrochemistry*, **37**, 833 (2001).
14. P. N. Bartlett, *Bioelectrochemistry. Fundamentals, Experimental Techniques and Applications*, John Wiley & Sons, Chichester (2008).
15. V. Flexer, K. F. E. Pratt, F. Garay, P. N. Bartlett, and E. J. Calvo, *Journal of Electroanalytical Chemistry*, **616**, 87 (2008).
16. G. Decher, *Science*, **277**, 1232 (1997).
17. E. J. Calvo, V. Flexer, M. Tagliazucchi, and P. Scodeller, *Physical Chemistry Chemical Physics*, **12**, 10033 (2010).
18. R. Szamocki, V. Flexer, L. Levin, F. Forchiasin, and E. J. Calvo, *Electrochimica Acta*, **54**, 1970 (2009).
19. P. Scodeller, F. J. Williams, and E. J. Calvo, *Analytical Chemistry*, **86**, 12180 (2014).
20. R. D. Milton, F. Giroud, A. E. Thumser, S. D. Minteer, and R. C. T. Slade, *Physical Chemistry Chemical Physics*, **15**, 19371 (2013).
21. R. D. Milton and S. D. Minteer, *Journal of the Electrochemical Society*, **161**, H3011 (2014).
22. L. Levin, F. Forchiassin, and A. Viale, *Process Biochemistry*, **40**, 1381 (2005).
23. C. Danilowicz, E. Corton, and F. Battaglini, *Journal of Electroanalytical Chemistry*, **445**, 89 (1998).
24. P. Scodeller, V. Flexer, R. Szamocki, E. J. Calvo, N. Tognalli, H. Troiani, and A. Fainstein, *Journal of the American Chemical Society*, **130**, 12690 (2008).
25. H. Bisswanger, *Enzyme Kinetics. Principles and Methods*, WILEY-VCH Verlag GmbH., Weinheim, Germany (2002).
26. P. N. Bartlett, C. S. Toh, E. J. Calvo, and V. Flexer, in *Bioelectrochemistry. Fundamentals, Experimental Techniques and Applications*, P. N. Bartlett Editor, p. 267, John Wiley & Sons, Chichester, UK (2008).
27. D. N. Blauch and J. M. Saveant, *Journal of the American Chemical Society*, **114**, 3323 (1992).
28. D. N. Blauch and J. M. Saveant, *Journal of Physical Chemistry*, **97**, 6444 (1993).
29. E. I. Solomon, A. J. Augustine, and J. Yoon, *Dalton Transactions*, 3921 (2008).
30. P. N. Bartlett and K. F. E. Pratt, *Journal of Electroanalytical Chemistry*, **397**, 61 (1995).
31. P. N. Bartlett and K. F. E. Pratt, *Biosensors & Bioelectronics*, **8**, 451 (1993).
32. V. Flexer, E. J. Calvo, and P. N. Bartlett, *Journal of Electroanalytical Chemistry*, **646**, 24.
33. A. Fersht, *Enzyme Structure and Mechanism*, w.h. Freeman and Co., Cambridge, UK (1985).
34. N. C. Price and L. sTEVENS, *Fundamentals of Enzymology*, Oxford University Press, Oxford (1996).
35. S. M. Jones and E. I. Solomon, *Cellular and Molecular Life Sciences*, **72**, 869 (2015).
36. L. S. Kau, D. J. Spirasolomon, J. E. Pennerhahn, K. O. Hodgson, and E. I. Solomon, *Journal of the American Chemical Society*, **109**, 6433 (1987).
37. U. M. Sundaram, H. H. Zhang, B. Hedman, K. O. Hodgson, and E. I. Solomon, *Journal of the American Chemical Society*, **119**, 12525 (1997).
38. R. Branden, Malmstro Bg, and T. Vanngard, *European Journal of Biochemistry*, **18**, 238 (1971).
39. C. D. Lubien, M. E. Winkler, T. J. Thamann, R. A. Scott, M. S. Co, K. O. Hodgson, and E. I. Solomon, *Journal of the American Chemical Society*, **103**, 7014 (1981).